

Junior Synonym of *Prosopocoilus blanchardi* (Coleoptera: Lucanidae) Proposed by the Integrated Taxonomic Approach¹

Shi-Ju Zhou, Yong-Jing Chen, Jing Liu, and Xia Wan²

Department of Ecology, School of Resources and Engineering, Anhui University, Jiulonglu Road 111, Anhui, Hefei 230601, China

J. Entomol. Sci. 54(4): 430–442 (October 2019)

Abstract The species *Prosopocoilus reni* Huang and Chen was discovered endemic to Hainan Island, the smallest and southernmost province of the People's Republic of China. The species is very similar to the widely distributed *Prosopocoilus blanchardi* (Parry) in China. In this study, we used the integrated approach to analyze the phylogenetic, genetic, geographic, and morphological data among *Prosopocoilus reni*, *P. blanchardi*, and some allied taxa from 43 specimens. The phylogenetic reconstruction indicated that *P. blanchardi* had divided into the eastern and western clades in China and *P. reni* was embedded in the two clades. The genetic distance implied that *P. reni* should not be a full species but an island population of *P. blanchardi* with deeply genetic isolation. The divergent time estimation further supported that *P. reni* was divergent from the eastern clade from Continental China, similar to another island population from Taiwan Island. The morphological comparisons among *P. reni*, *P. blanchardi*, and other allied species showed that the key diagnosed character of *P. reni* should be phenotypic variation as a tropical island population. Therefore, the species *P. reni* was proposed as a new junior synonym of *P. blanchardi* based on the integrated taxonomy analysis.

Key Words *Prosopocoilus reni*, new junior synonym, phylogeny, integrated taxonomy

The species of *Prosopocoilus blanchardi* (Parry) was originally described from Mongolia by Parry in 1873. The taxonomic status of *P. blanchardi* had been downgraded to one of a subspecies of the *Prosopocoilus astacoides* (Hope) species group (Fujita 2010; Huang and Chen 2011, 2013; Mizunuma and Nagai 1994). In this study, we still treat it as a full species due to the lack of detailed discussion in the previous status change.

Prosopocoilus blanchardi is an easily recognizable stag beetle in the field due to the following morphological characteristics (Fig. 1A, B): (a) Body is stout, dorsal surface is brown to yellow-brown and the head and pronotum with more-deeper color; the pronotum with a narrowly middle stripe (sometimes quite faint) and a small dark spot on each side; (b) the head's broad, frontal region is deeply concaved, the vertex raised with a pair of bluntly triangular projection in males whereas the head is small, relatively flattened, without any projection in females; (c) in large- and medium-sized males, the mandibles developed strongly incurved,

¹Received 28 September 2018; accepted for publication 15 January 2019.

²Corresponding author (Email: wanxia@ahu.edu.cn).

more than three times as long as that of the head in length, each side with a sharp large inner tooth near to the base (sometimes at the middle) and four much smaller inner teeth near to the apex; in small males, the mandibles are slightly curved, the length is no more than two times that of the head, each side with a very small basal denticle and 3–4 small denticles near to the apex. So far, this species has been known as widely distributed in Mongolia, the vast area of the Mainland China, Jeju Island, and Taiwan Island (Fig. 2) (Bartolozzi and Sprecher–Uebersax 2006; Kim and Kim 2010; Wan 2007).

Another Chinese species, *Prosopocoilus reni* that is endemic to Hainan Island was similar to *Prosopocoilus astacoides* (which probably meant that *P. reni* Huang and Chen was similar to nine subspecies in this species group according to the descriptions of Huang and Chen (2011, 2013). It could be identified by the following characters: (a) the body mostly black on both dorsal and ventral surfaces; (b) the head and pronotum more coarsely punctured; the projection of the head in the larger-sized males broader and blunter at apex; (c) aedeagus stouter with the basal piece wider in dorsal or ventral view; (d) the 9th hemisternite of the female genitalia markedly broader and plate-like, and sclerotized on part of the hemisternite with the inner lateral margin less concaved (Fig. 1A, B).

Considering the intraspecifically morphological complexity in Lucanidae, such as remarkable sexual dimorphism, male polymorphism, phenotypical color pattern, and variation in different geographic populations, the taxonomic position of *P. reni* is worthy of serious discussion with integrated approaches. In our opinion, *P. reni* may be more similar to *P. blanchardi*; the differences between the two species are negligible and hardly any diagnostic character was found to distinguish them except for that *P. reni* has the unstable black color of the entire body. We needed to further reveal the relationship between the two species. Therefore, this study was conducted to present phylogenetic inferences based on COI and 16S rDNA genes of the two species from 10 localities (calibration time in these species was analyzed based on COI and 16S rDNA genes to delineate their possible differentiation histories) and to calculate the intraspecific and interspecific genetic distances of the two mitochondrial genes, if the two taxa can be distinguished.

Materials and Methods

Sample collection. Forty-two *Prosopocoilus* stag beetles were collected including 34 samples of the ingroup (26 *P. blanchardi* collected from 9 geographic localities, 8 *P. reni* from the type locality of Hainan Island), and 8 samples of the outgroup (1 each of *Prosopocoilus forficula* (Thomson), *Prosopocoilus spineus* (Didier), *Prosopocoilus suturalis* (Olivier), and 5 *Prosopocoilus kachinensis* Bomans & Miyashita) (Table 1). Voucher specimens and their extracted genomic DNA are deposited in the research collection at the Museum of Anhui University, China.

DNA extraction, amplification, and sequencing. The specimens were preserved in 100% ethanol at -20°C for molecular analyses. A small portion of the muscle from a specimen was used for total DNA extraction with the Blood and Tissue Kit (Qiagen, Germany). The primer sets used to amplify two mitochondrial genes, COI and 16S rDNA, are listed in Table 2. PCR amplification reactions were conducted in 25- μL volumes containing 10 μM of each primer (forward and reverse)

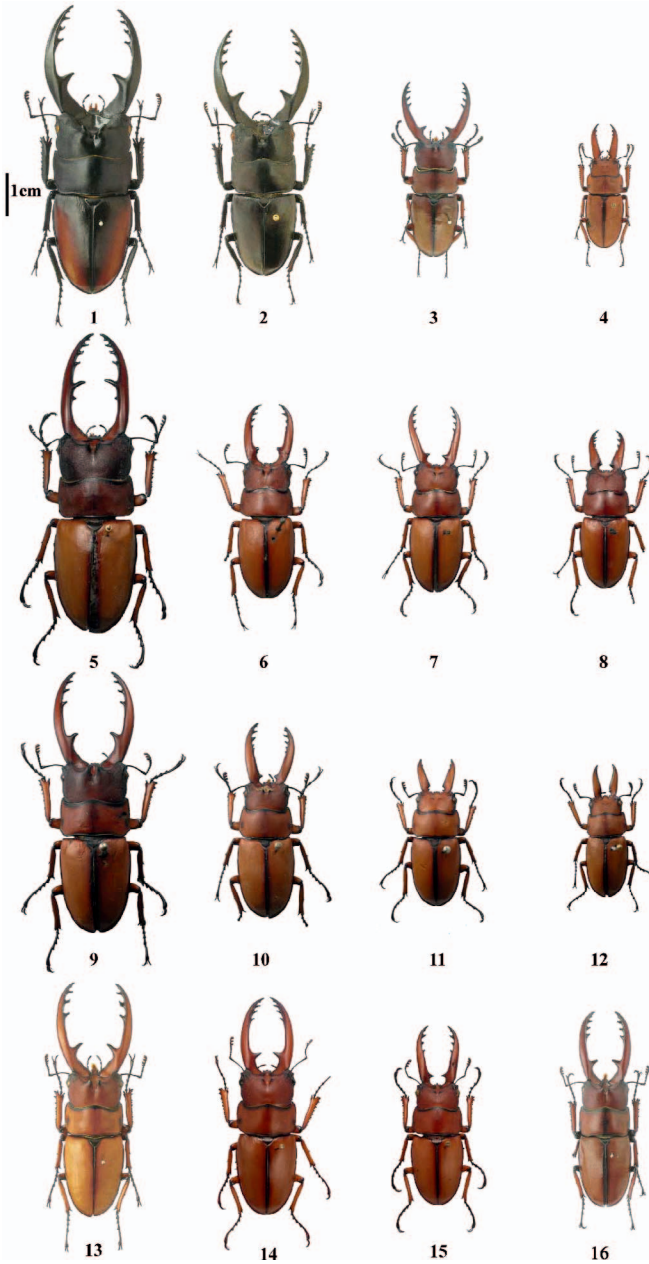


Fig. 1. (A) Habitus of *Prosopocoilus reni* and *Prosopocoilus blanchardi* (male) in dorsal view. 1, 2: *P. reni* (see the PL.37, figures 35–5, 4 in the book of Huang and Chen, 2013); 3, 4: *P. blanchardi*_TM (see the PL.34, figures 34–66, 62 in the book of Huang and Chen, 2013); 5, 6, 7, 8: *P. blanchardi*_TW; 9, 10, 11, 12: *P. blanchardi*_BX; 13: *P. blanchardi*_QL

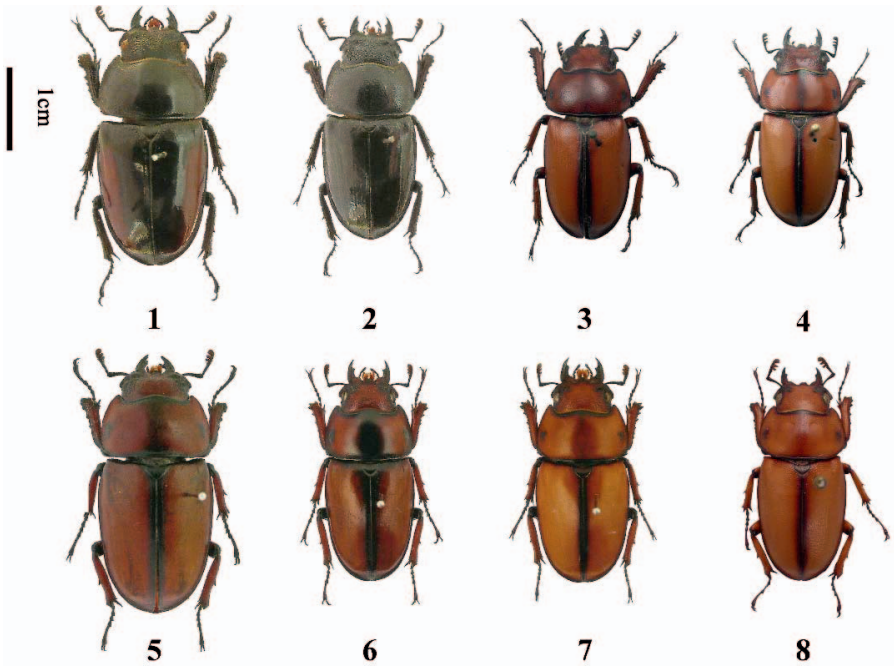


Fig. 1. Continued.

2 μL template DNA, 12.5 μL 2 \times EasyTaq SuperMix (+dye), and 8.5 μL sterile, double-distilled water (ddH₂O) to make up a final volume of 25 μL . The PCR amplifications were performed under the following conditions: an initial denaturation at 94°C for 2 min followed by 35–37 cycles of denaturation at 94°C for 40 s, annealing at 52–58°C for 50 s, and elongation at 70°C for 1 min, then a final extension step at 72°C for 7 min. The temperature of annealing was determined by the length of fragments. Amplifications were purified using Template DNA Amplify Kit (Ensure Biologicals). For sequencing, we used the ABI PRISM BigDye Terminator version 3.1 Cycle Sequencing Kit (Life Technologies, USA) and cycle sequencing reactions were performed on ABI PRISM 3730xl automated sequenc-

(see the PL.34, figures 34–72 in the book of Huang and Chen, 2013); 14, 15: *P. blanchardi*_QLI; 16: *blanchardi*_DL (see the PL.34, figures 34–71 in the book of Huang and Chen, 2013). (B) Habitus of *P. reni* and *P. blanchardi* (female) in dorsal view. 1, 2: *P. reni* (see the PL.37, figures 35–3, 1 in the book of Huang and Chen, 2013); 3: *P. blanchardi*_TW; 4: *P. blanchardi*_BX; 5: *P. blanchardi*_TM (see the PL.36, figures 34–20 in the book of Huang and Chen, 2013); 6: *P. blanchardi*_DL (see the PL.36, figures 34–77 in the book of Huang and Chen, 2013); 7: *P. blanchardi*_QL (see the PL.36, figures 34–76 in the book of Huang and Chen, 2013); 8: *P. blanchardi*_QLI.

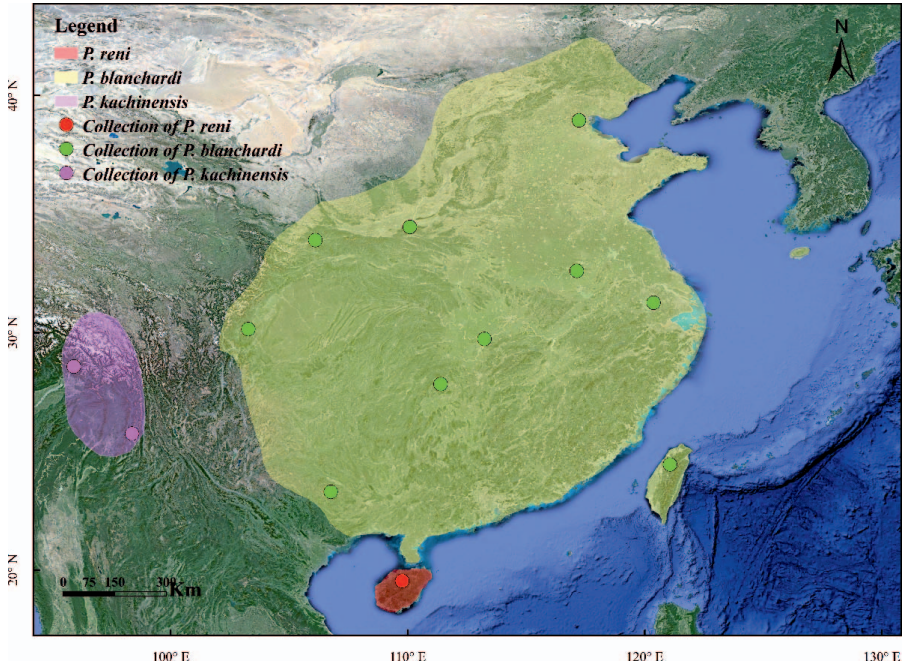


Fig. 2. Collection and distribution of *Prosopocoilus reni*, *Prosopocoilus blanchardi*, *Prosopocoilus kachinensis*. The map is generated using the software ArcGIS 10.3 (<http://www.esri.com/software/arcgis>) based on the geospatial data from the National Geomatics Center of China.

ers (Life Technologies) at Sangon Biotech Company, China. The sequences were submitted to GenBank under various accession numbers (Table 1).

Nucleotide sequence alignment, phylogenetic analyses, and genetic distances. Sequences were assembled in Geneious version 9.0.5 (Biomatters Ltd., New Zealand). To test whether the coding gene (COI) was successfully translated before aligned in MEGA v. 6.05 (Tamura et al. 2013), all sequences were aligned using the automatically selected algorithm in MAFFT v. 7.017 with the default alignment parameters (Kato et al. 2002, Kato and Toh 2008). The resulting aligned sequence matrices were masked using Gblocks v. 0.91b (Castresana 2000; Talavera and Castresana 2007). Divergences among taxa were analyzed using MEGA v. 6.0 p-distance. DNA sequences COI (a total of 43) of *Prosopocoilus* were assembled for genetic distance analyses.

Phylogenetic inference was based on two molecular markers using maximum likelihood (ML) and Bayesian inference (BI) methods. Bayesian analysis was implemented in MrBayes v. 3.2 (Ronquist et al. 2012) assigning site-specific models. Models of nucleotide substitution were selected according to the Akaike Information Criterion (AICc) with Partitionfinder v. 2.1.1 (Lanfear et al. 2012). The COI dataset was divided into three partitions by codon position (pos1–3), and PartitionFinder v. 2.1.1 was used to determine the best-fitting models for each

partition. The best-fitting models were as follows: COI_pos1, SYM + I; COI_pos2, HKY + I; COI_pos3, GTR+I+G; and 16S rRNA, GTR+G. Maximum likelihood phylogenetic inference analyses were implemented in RAxML v. 3. (Stamatakis 2014) under the GTR+I+G model. For bootstrapping, we performed 1,000 ML pseudo-replicates analyses. Bayesian inference was conducted using MrBayes v. 3.2 with two simultaneous runs of 3×10^7 generations. Samples were drawn every 1,000 Markov Chain Monte Carlo (MCMC) step, with the first 25% discarded as burn-in. The average standard deviation of split frequencies should be less than 0.01.

Divergence time analysis. Divergence time was estimated with a strict molecular clock model (Drummond and Rambaut 2007) in BEAST v. 2.1.3 (Bouckaert et al. 2014). The MCMC chain was run for 3×10^7 generations with four independent runs. Substitution rates of 1.77% per lineage in million years (Myr) for COI combining with 0.54%/lineage/Myr for 16S rDNA have been suggested optimally for beetles (Papadopoulou et al. 2010). The resultant BEAST log files were viewed using Tracer v. 1.6 (Rambaut et al. 2014) to analyze the output results of the effective sample size (ESS) for the posterior distribution of estimated parameter values. With a 25% burn-in threshold, all post-burn-in trees from the four independent runs were combined using the software log combiner v. 2.1.2 (Bouckaert et al. 2014). Tree annotator v. 2.1.2 (Bouckaert et al. 2014) was used to summarize information (i.e., Nodal posterior probabilities, posterior estimates, and highest posterior density limits) from the individual post-burn-in trees onto a single maximum clade credibility (MCC) tree. The summarized information was visualized on the MCC tree using Figtree v. 1.4.3 (Rambaut 2016).

Results

Forty-two new COI and 16S rDNA sequences were obtained in this study (Table 1). The analysis under Bayesian inference converged well, as indicated by an average standard deviation of split frequency of 0.0004255 after removing burn-in samples. All parameters had ESS values above 200.

The phylogenetic analyses under both Bayesian inference and the ML inference overall recovered the identical topology with a highly supported backbone (Fig. 3). All analyses showed that populations of *P. blanchardi* formed four separate monophyletic clades consisting of individuals from ESI (BX-DL-DBE-TM), ESII (TW), WSI (DB-QL-QLI) and WSII (QLG). *Prosopocoilus reni* was found to be embedded within ESI, ESII, WSI, and WSII of *P. blanchardi*.

The genetic distances (K2P-distances) using the COI gene were calculated among all the taxa. As a result, the value was 0.049 in minimum among ESI-ESII and 0.121 in maximum among WSI-ESII in *P. blanchardi*. This was 0.089 in minimum and 0.149 in maximum between *P. reni* and *P. blanchardi* (Table 3), which were much lower than the minimum value 0.205 among of interspecific taxa in *Prosopocoilus* (Table 3).

The mean divergence age estimates and 95% HPDs for nodes of interest based on the BEAST analysis are presented in Fig. 4. The crown age of the outgroup (*P. forficular*) and other ingroup members occurred at the Early Miocene 21.4 Mya (95% HPD: 15.6–30.1 Mya, node 1). The sister species *P. kachinensis* diverged

Table 1. Location and GenBank accession numbers of specimens. For the convenience of the study, we abbreviate nine geographic localities of *Prosopocoilus blanchardi* as *P. blanchardi*_BX (collected from Baxian Mountain), *P. blanchardi*_DB (collected from Daba Mountain), *P. blanchardi*_DBE (collected from Dabie Mountain), *P. blanchardi*_DL (collected from Dalou Mountain), *P. blanchardi*_QLG (collected from Qinglong Mountains), *P. blanchardi*_QL (collected from Qinling Mountains), *P. blanchardi*_QLI (collected from Qionglai Mountains), *P. blanchardi*_TW (collected from Taiwan Island), and *P. blanchardi*_TM (collected from Tianmu Mountain).

| No. | Species | Location | (COI) Accession No. | (16S) Accession No. |
|-----|----------------------------|--------------------------|---------------------------|---------------------------|
| 1 | <i>P. blanchardi</i> _P006 | Baxian Mountain (BX) | MH365392 | MH365350 |
| 2 | <i>P. blanchardi</i> _P008 | Baxian Mountain (BX) | MH365393 | MH365351 |
| 3 | <i>P. blanchardi</i> _P009 | Baxian Mountain (BX) | MH365394 | MH365352 |
| 4 | <i>P. blanchardi</i> _P010 | Daba Mountain (DB) | MH365395 | MH365353 |
| 5 | <i>P. blanchardi</i> _P011 | Dalou Mountain (DL) | MH365396 | MH365354 |
| 6 | <i>P. blanchardi</i> _P012 | Taiwan Island (TW) | MH365397 | MH365355 |
| 7 | <i>P. blanchardi</i> _P013 | Taiwan Island (TW) | MH365398 | MH365356 |
| 8 | <i>P. blanchardi</i> _P014 | Taiwan Island (TW) | MH365399 | MH365357 |
| 9 | <i>P. blanchardi</i> _P015 | Taiwan Island (TW) | MH365400 | MH365358 |
| 10 | <i>P. blanchardi</i> _P016 | Taiwan Island (TW) | MH365401 | MH365359 |
| 11 | <i>P. blanchardi</i> _P062 | Dabie Mountain (DBE) | MH365402 | MH365360 |
| 12 | <i>P. blanchardi</i> _P063 | Dabie Mountain (DBE) | MH365403 | MH365361 |
| 13 | <i>P. blanchardi</i> _P064 | Qionglai Mountains (QLI) | MH365404 | MH365362 |
| 14 | <i>P. blanchardi</i> _P065 | Qionglai Mountains (QLI) | MH365405 | MH365363 |
| 15 | <i>P. blanchardi</i> _P066 | Qionglai Mountains (QLI) | MH365406 | MH365364 |
| 16 | <i>P. blanchardi</i> _P078 | Dalou Mountain (DL) | MH365407 | MH365365 |
| 17 | <i>P. blanchardi</i> _P091 | Dabie Mountain (DBE) | MH365408 | MH365366 |
| 18 | <i>P. blanchardi</i> _P092 | Dabie Mountain (DBE) | MH365409 | MH365367 |
| 19 | <i>P. blanchardi</i> _P093 | Dabie Mountain (DBE) | MH365410 | MH365368 |
| 20 | <i>P. blanchardi</i> _P094 | Dabie Mountain (DBE) | MH365411 | MH365369 |
| 21 | <i>P. blanchardi</i> _P095 | Tianmu Mountain (TM) | MH365412 | MH365370 |
| 22 | <i>P. blanchardi</i> _P096 | Tianmu Mountain (TM) | MH365413 | MH365371 |
| 23 | <i>P. blanchardi</i> _P097 | Qinling Mountains (QL) | MH365414 | MH365372 |

Table 1. Continued.

| No. | Species | Location | (COI) Accession No. | (16S) Accession No. |
|-----|-----------------------------|--------------------------|---------------------------|---------------------------|
| 24 | <i>P. blanchardi</i> _P098 | Qinling Mountains (QL) | MH365415 | MH365373 |
| 25 | <i>P. blanchardi</i> _P119 | Qinglong Mountains (QLG) | MH365416 | MH365374 |
| 26 | <i>P. blanchardi</i> _P120 | Qinglong Mountains (QLG) | MH365417 | MH365375 |
| 27 | <i>P. reni</i> _P005 | Hainan Island | MH365424 | MH365382 |
| 28 | <i>P. reni</i> _P037 | Hainan Island | MH365425 | MH365383 |
| 29 | <i>P. reni</i> _P038 | Hainan Island | MH365426 | MH365384 |
| 30 | <i>P. reni</i> _P039 | Hainan Island | MH365427 | MH365385 |
| 31 | <i>P. reni</i> _P047 | Hainan Island | MH365428 | MH365386 |
| 32 | <i>P. reni</i> _P048 | Hainan Island | MH365429 | MH365387 |
| 33 | <i>P. reni</i> _P049 | Hainan Island | MH365430 | MH365388 |
| 34 | <i>P. reni</i> _P050 | Hainan Island | MH365431 | MH365389 |
| 35 | <i>P. kachinensis</i> _P022 | Hengduan Mountains | MH365419 | MH365377 |
| 36 | <i>P. kachinensis</i> _P023 | Hengduan Mountains | MH365420 | MH365378 |
| 37 | <i>P. kachinensis</i> _P052 | Himalayas | MH365421 | MH365379 |
| 38 | <i>P. kachinensis</i> _P053 | Himalayas | MH365422 | MH365380 |
| 39 | <i>P. kachinensis</i> _P054 | Himalayas | MH365423 | MH365381 |
| 40 | <i>P. forcifula</i> _Q5 | Tianmu Mountain | MH365418 | MH365376 |
| 41 | <i>P. spineus</i> _Q6 | Qinglong Mountains | MH365433 | MH365391 |
| 42 | <i>P. confucius</i> _Q7 | Tianmu Mountain | KU552119 | KU552119 |
| 43 | <i>P. suturalis</i> _Q10 | Qinglong Mountains | MH365432 | MH365390 |

Table 2. PCR primers.

| Gene | Primer | Sequence 5'→3' | References |
|---------------------------|------------|---------------------------|--------------------|
| <i>COI</i> | C1-J-2183 | CAACATTTATTTTGATTTTTTGG | Simon et al. 1994 |
| | TL2-N-3014 | TCCAATGCACTAATCTGCCATATTA | Simon et al. 1994 |
| <i>16S</i> <i>rDNA</i> | 16S-F1 | CCGGTTTGAAGCTCAGATCATG | Hosoya et al. 2001 |
| | 16S-R1 | TAATTTATTGTACCTTGTGTATCAG | Hosoya et al. 2001 |

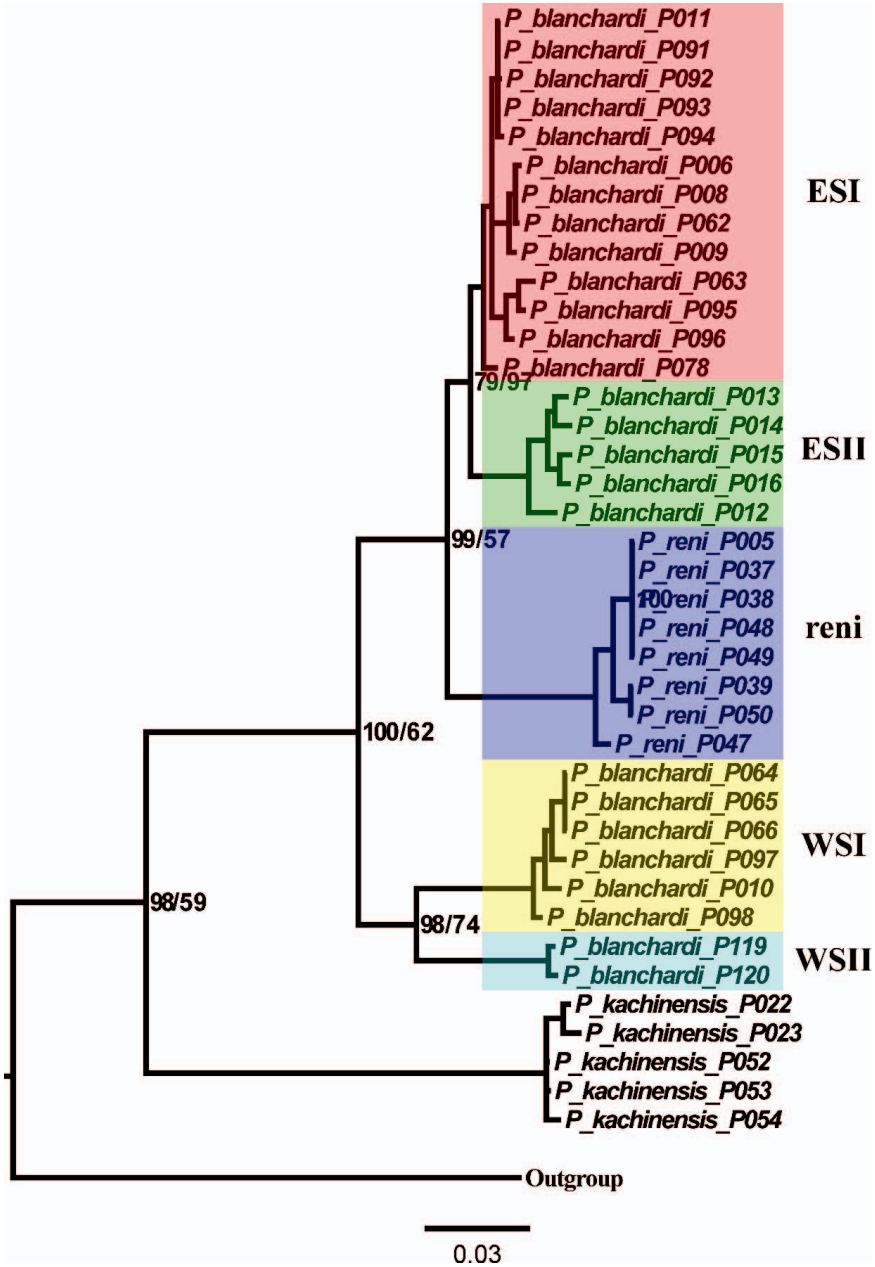


Fig. 3. Phylogenetic inferences based on COI+16S rDNA using Bayesian inference (BI). Both bootstrapping values of BI (left) and posterior probabilities of maximum likelihood (ML) (right) are shown at nodes.

Table 3. Interspecific pairwise comparison using p-distance based on COI for five *Prosopocoilus* taxa and intraspecific pairwise comparison using p-distance based on COI for the five groups forming the BI and ML *blanchardi-reni* clades.

| Groups* | SP | CO | SU | FO | KA | WSI | WSII | ESII | ESI | RE |
|---------|-------|-------|-------|-------|-------|-------|-------|-------|-------|----|
| SP | | | | | | | | | | |
| CO | 0.227 | | | | | | | | | |
| SU | 0.260 | 0.210 | | | | | | | | |
| FO | 0.221 | 0.233 | 0.232 | | | | | | | |
| KA | 0.228 | 0.241 | 0.231 | 0.205 | | | | | | |
| WSI | 0.249 | 0.252 | 0.221 | 0.203 | 0.180 | | | | | |
| WSII | 0.238 | 0.255 | 0.225 | 0.187 | 0.174 | 0.104 | | | | |
| ESII | 0.251 | 0.253 | 0.212 | 0.206 | 0.185 | 0.121 | 0.119 | | | |
| ESI | 0.245 | 0.241 | 0.213 | 0.200 | 0.169 | 0.112 | 0.114 | 0.049 | | |
| RE | 0.240 | 0.219 | 0.202 | 0.179 | 0.174 | 0.149 | 0.129 | 0.095 | 0.089 | |

* SP, *P. spineus*; CO, *P. confucius*; SU, *P. suturalis*; FO, *P. forficula*; KA, *P. kachinensis*; RE, *P. reni*.

from the lineage of “*P. reni-P. blanchardi*” at the Middle Miocene 14.7 Mya (95% HPD: 10.0–22.4 Mya, node 2). Within the lineage of “*P. reni-P. blanchardi*,” the age estimate of the crown node for the western and eastern clade was dated to be 6.9 Mya (95% HPD: 4.6–10.6 Mya, node 3) in the Late Miocene. The crown age of the western clade was estimated to be 5.2 Mya (95% HPD: 3.2–9.2 Mya; node 4) in the Late Miocene/Pliocene interface. That of the eastern clade was at 3.9 Mya (95% HPD: 2.4–6.2 Mya; node 5) in the Pliocene. Within the eastern clade, the divergent time between the subclade from the Continental China (ESI) and the subclade from Taiwan Island (ESII) was 2.3 Mya during the Early Pleistocene (95% HPD: 1.3–4.0 Mya, node 6).

Discussion

The identical topology of phylogenetic analyses strongly supported that *P. kachinensis* was sister to *P. blanchardi*. However, the paraphyletic relationship of *P. reni* implied that its full morph-species position should be dubious. The K2P-distance further indicated *P. reni* most likely represented an island population of *P. blanchardi*, similar to those members distributed in Taiwan Island. Thus, phylogenetic analyses and genetic distance both suggested that “*P. reni-P. blanchardi*” could divide into two clades: the “Eastern Clade” consisting of the three subclades of ESI, ESII, and *reni* and the “Western Clade” consisting of two subclades of WSI and WSII. The western and eastern clade being monophyletic was also a cue that *P. reni* should be another island population of *P. blanchardi* with clear differentiation.

Morphologically, *P. reni* was also highly similar to *P. blanchardi*, although there were the following characters from Huang and Chen (2011, 2013): dorsal surfaces almost black; the frontal projections on the head broader and blunter at apex in larger-sized males; the aedeagus of male genitalia more stout, the 9th hemisternite of the female genitalia more broad. Nevertheless, characters of body color, head including mandibles, and female genitalia often display remarkably phenotypic variation in stag beetles (Holloway 2007). In comparison, the “distinction” of *P. reni* with those of allied taxa in the *P. astacoides* species group, and these “differences,” should not be the criteria for the identification of full species but of the intraspecific variation. Actually, the images of *P. reni* and *P. blanchardi* in Huang and Chen (2013) exhibited these variations. In *P. reni*, some individuals are uniformly black and some are partly dimly reddish on the elytra (Fig. 1A, B); in *P. blanchardi*, the frontal projections showed the variety ranged from “broader-blunter,” “broader-sharper,” and “narrower-sharper” (Fig. 1A, B). Consequently, the characters of *P. reni* should be within the scope of phenotypic variations of *P. blanchardi*.

Overall, we analyzed the integrated data from the phylogeny, genetic distance, divergent time, and morphological comparison of the representative populations of *P. blanchardi* and *P. reni*. The results indicated that *P. blanchardi* was widely distributed in China, with a remarkable break between the western and eastern region, and the eastern clades also included the Taiwan Island and Hainan Island populations with deep genetic isolation. Therefore, we propose *P. reni* as a junior synonym of *P. blanchardi*, taxonomically, due to the fact that the name exactly represents the Hainan Island population of *P. blanchardi*. During this study, we also found that several other allied taxa of *P. blanchardi* remain to be studied due to their morphological similarities and confused taxonomic changes without sufficient evidences. We hope that a comprehensive work can be conducted later in consideration that these taxa are ideal models for understanding the high biodiversity of beetles.

Acknowledgments

This work was supported by research grants from the National Natural Science Foundation of China (No. 31201745, No. 31071954, and No. 31572311). We thank Hu Li and Fan Song (Department of Entomology, China Agricultural University, west Campus) who gave us invaluable advice on data analysis during this study. We also express our gratitude to lab colleagues, Qian Wang and Zi-qi Lin, for their kind help.

References Cited

- Bartolozzi, L. and E. Sprecher-Uebersax. 2006.** Lucanidae, Pg. 63–76. *In* Lobl, I., Smetana, A. (eds.), Catalogue of Palaearctic Coleoptera. Volume 3: Scarabaeoidea - Scirtoidea - Dascilloidea - Buprestoidea - Byrrhoidea. Apollo Books, Brooklyn, NY.
- Bouckaert, R., J. Heled, D. Kühnert, T. Vaughan, C.H. Wu, D. Xie, M.A. Suchard, A. Rambaut and A.J. Drummond. 2014.** Beast 2: A software platform for Bayesian evolutionary analysis. *PLoS Comput. Biol.* 10: e1003537.
- Castresana, J. 2000.** Selection of conserved blocks from multiple alignments for their use in phylogenetic analysis. *Mol. Biol. Evol.* 17: 540–552.
- Chiang, T.Y. and B.A. Schaal. 2006.** Phylogeography of plants in Taiwan and the Ryukyu Archipelago. *Taxon* 55: 31–41.
- Drummond, A.J. and A. Rambaut. 2007.** Beast: Bayesian evolutionary analysis by sampling trees. *BMC Evol. Biol.* 7: 214.

- Fujita, H. 2010.** The Lucanid beetles of the world, Pg. 1–488. *In* Mushi-Sha's Iconographic Series of Insects. Volume 6. Mushi-sha, Tokyo.
- Holloway, B.A. 2007.** Lucanidae (Insecta: Coleoptera), Pg. 1–254. *In* Duval C.T., Crosby T.K., Zhang Z.Q. (eds.), Fauna New Zealand. Manaaki Whenua Press (Auckland).
- Hosoya, T., M. Honda and K. Araya. 2001.** Genetic variations of 16S rRNA gene observed in *Ceruchus lignarius* and *Dorcus rectus rectus* (Coleoptera: Lucanidae). *Entomol. Sci.* 4: 335–344.
- Huang, H. and C.C. Chen. 2011.** Notes on *Prosopocoilus* Hope (Coleoptera: Scarabaeoidea: Lucanidae) from China, with the description of two new species. *Zootaxa* 3126: 39–54.
- Huang, H. and C.C. Chen. 2013.** Stag Beetles of China II. Formosa Ecological Co., New Taipei, Taiwan.
- Katoh, K., K. Misawa, K. Kuma and T. Miyata. 2002.** MAFFT: A novel method for rapid multiple sequence alignment based on fast Fourier transform. *Nucleic Acids Res.* 30: 3059–3066.
- Katoh, K. and H. Toh. 2008.** Recent developments in the MAFFT multiple sequence alignment program. *Brief. Bioinform.* 9: 286–298.
- Kim, J.I. and S.Y. Kim. 2010.** Review of family Lucanidae in Korea with the description of one new species. *Entomol. Res.* 40: 55–81.
- Lanfear, R., B. Calcott, S.Y. Ho and S. Guindon. 2012.** Partitionfinder: Combined selection of partitioning schemes and substitution models for phylogenetic analyses. *Mol. Biol. Evol.* 29: 1695–1701.
- Meng, H.H., X.Y. Gao, J.F. Huang and M.L. Zhang. 2015.** Plant phylogeography in arid Northwest China: Retrospectives and perspectives. *J. Syst. Evol.* 53: 33–46.
- Mizunuma, T. and S. Nagai. 1994.** The lucanid beetles of the world, Pg. 1–340. *In* Fujita, H. (ed.), Mushisha Iconographic Series of Insects 1. Mushi-sha (Tokyo).
- Papadopoulou, A., I. Anastasiou and A.P. Vogler. 2010.** Revisiting the insect mitochondrial molecular clock: The mid-Aegean trench calibration. *Mol. Biol. Evol.* 27: 1659–1672.
- Qiu, Y., Q. Lu, Y. Zhang and Y. Cao. 2017.** Phylogeography of East Asia's tertiary relict plants: Current progress and future prospects. *Biodivers. Sci.* 25: 136–146.
- Rambaut, A. 2016.** FigTree: Tree figure drawing tool, version 1.4.3. Institute of Evolutionary Biology, Univ. of Edinburgh, <http://tree.bio.ed.ac.uk/>.
- Rambaut, A., M.A. Suchard, D. Xie and A.J. Drummond. 2014.** Tracer v1.6. <http://beast.bio.ed.ac.uk/Tracer>.
- Ronquist, F., M. Teslenko, P.V.D. Mark, D.L. Ayres, A. Darling, S. Höhna, B. Larget, L. Liu, M.A. Suchard and J.P. Huelsenbeck. 2012.** MrBayes 3.2: Efficient Bayesian phylogenetic inference and model choice across a large model space. *Syst. Biol.* 61: 539–542.
- Sibuet, J.C. and S.K. Hsu. 2004.** How was Taiwan created? *Tectonophysics* 379: 159–181.
- Simon, C., F. Frati, A. Beckenbach, B. Crespi, H. Liu and P. Flook. 1994.** Evolution, weighting, and phylogenetic utility of mitochondrial gene sequences and a compilation of conserved polymerase chain reaction primers. *Ann. Entomol. Soc. Am.* 87: 651–701.
- Stamatakis, A. 2014.** Raxml version 8: A tool for phylogenetic analysis and post-analysis of large phylogenies. *Bioinformatics* 30: 1312–1313.
- Talavera, G. and J. Castresana. 2007.** Improvement of phylogenies after removing divergent and ambiguously aligned blocks from protein sequence alignments. *Syst. Biol.* 56: 564–577.
- Tamura, K., G. Stecher, D. Peterson, A. Filipksi and S. Kumar. 2013.** MEGA6: Molecular Evolutionary Genetics Analysis version 6.0. *Mol. Biol. Evol.* 30: 2725–2729.
- Wan, X. 2007.** Study on the systematics of Lucanidae from China (Coleoptera: Scarabaeoidea), MS Thesis, Institute of Zoology, Chinese Academy of Sciences, Beijing.
- Ye, J.W., Y. Zhang and X.J. Wang. 2017.** Phylogeographic breaks and the mechanisms of their formation in the Sino-Japanese floristic region. *J. Plant Ecol.* 41: 1003–1019.
- Zhou, Z., J. Huang and W. Ding. 2017.** The impact of major geological events on Chinese flora. *Biodivers. Sci.* 25: 17–23.
- Zhu, H. 2016.** Biogeographical evidences help revealing the origin of Hainan Island. *PLoS ONE* 11: e0151941.